

# Scaling Laws for Black-box Adversarial Attacks

Chuan Liu<sup>1,2,3\*</sup> Huanran Chen<sup>1,3\*</sup> Yichi Zhang<sup>1,3</sup> Yinpeng Dong<sup>1,3</sup> Jun Zhu<sup>1,3</sup>

<sup>1</sup> Dept. of Comp. Sci. and Tech., Institute for AI, Tsinghua-Bosch Joint ML Center, THBI Lab, BNRist Center, Tsinghua University, Beijing, 100084, China

<sup>2</sup> IIS, Tsinghua University <sup>3</sup> RealAI

{liuchuan22, zyc22}@mails.tsinghua.edu.cn, huanran.chen@outlook.com

{dongyinpeng, dcszj}@mail.tsinghua.edu.cn

## Abstract

A longstanding problem of deep learning models is their vulnerability to adversarial examples, which are often generated by applying imperceptible perturbations to natural examples. Adversarial examples exhibit cross-model transferability, enabling to attack black-box models with limited information about their architectures and parameters. Model ensembling is an effective strategy to improve the transferability by attacking multiple surrogate models simultaneously. However, as prior studies usually adopt few models in the ensemble, there remains an open question of whether scaling the number of models can further improve black-box attacks. Inspired by the findings in large foundation models, we investigate the scaling laws of black-box adversarial attacks in this work. By analyzing the relationship between the number of surrogate models and transferability of adversarial examples, we conclude with clear scaling laws, emphasizing the potential of using more surrogate models to enhance adversarial transferability. Extensive experiments verify the claims on standard image classifiers, multimodal large language models, and even proprietary models like GPT-4o, demonstrating consistent scaling effects and impressive attack success rates with more surrogate models. Further studies by visualization indicate that scaled attacks bring better interpretability in semantics, indicating that the common features of models are captured.

## 1. Introduction

Over the past decade, deep learning has achieved remarkable advancements across various computer vision tasks, leading to its widespread application in practical contexts [52]. However, deep neural networks (DNNs) remain susceptible to adversarial examples [33, 76] – perturbations that are subtle and nearly imperceptible but can significantly

\*Equal contribution.

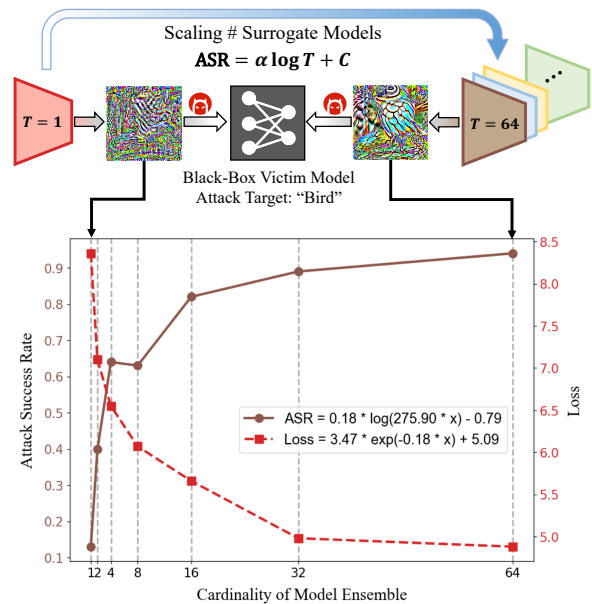


Figure 1. Key insights of our scaling laws for the transfer-based black-box attack regarding the number of surrogate models. By scaling the model ensembling, we observe that the attack success rate (ASR) and the discriminative loss on the target model follow the scaling laws, and these two metrics have a clear symmetry between each other. As the cardinality of models scales, the semantic interpretability of the adversarial perturbations keeps increasing by visualization. Details of our analyses are shown in Sec. 4.

mislead the model, resulting in incorrect predictions. Adversarial attack has garnered a considerable interest due to its implications for understanding DNN functionality [23], assessing model robustness [100], and informing the development of more secure algorithms [63].

Adversarial attacks are typically categorized into white-box and black-box attacks. Given the greater risks with commercial services, e.g., GPT-4 [66], black-box attack

methodologies [24, 54] have become a growing focus. One prominent approach within black-box attacks is the transfer-based attack, which approximately optimizes the adversarial examples against the black-box model by minimizing the discriminative loss on a selection of predefined surrogate models. Researchers have devised advanced optimization algorithms [54, 63, 85] and data augmentation techniques [25, 61] in the context of transfer attacks. Model ensembling [24, 58] further facilitates these methods by leveraging multiple surrogate models simultaneously to improve the robustness of adversarial examples. By averaging the gradients or predictions from different models, ensemble attack methods seek to increase the transferability across various target models [13, 24].

Despite the progress in ensemble attack algorithms, the number of surrogate models used is often limited, leaving the concept of model ensemble scaling under-explored. In contrast to prior works, we hereby investigate the scaling laws of ensemble attacks. Notably, the concept of scaling laws has led to substantial advancements in pretrained models, exemplified by the development of the Generative Pre-trained Transformer (GPT) [46]. Traditional scaling laws aim for better generalization to unseen scenarios by training on massive data, while ensemble attacks perform optimization on multiple models for better transferability. These two claims are indeed equivalent as prior works [13, 24] have pointed out that the transferability of adversarial examples generated from surrogate models parallels the generalization observed in neural network training. This equivalence prompts an intriguing question: *Can we achieve significant improvements in transfer-based attack by scaling the number of surrogate models, akin to the scaling of data and model parameters in GPT?*

In this study, we establish the scaling laws of black-box ensemble attacks regarding the number of surrogate models. We first perform a theoretical analysis on the convergence of ensemble attacks, which motivates our further empirical studies. By conducting extensive experiments of targeted attacks, we systematically explore the scaling of model ensembling, uncovering clear trends that inform our understanding of scaling behavior in ensemble attacks. Besides near 100% attack success rates against black-box classifiers, we also frequently mislead the predictions of modern Vision Language Models (VLMs) to predefined objects, solely with a set of pretrained classification models.

Beyond these studies on open-source models, we leverage our insights to conduct scaled attacks on proprietary models like GPT-4 [66]. We extend the attack methods to a group of CLIP vision encoders to craft targeted adversarial examples, which achieve a success rate of 90% against GPT-4o and GPT-4-Turbo, and over 60% against other commercial MLLMs. This highlights the vulnerabilities of these models to perturbations and the significance of the scaling

laws for ensemble attack. We also explain the existence of the scaling laws in ensemble attacks from two aspects via further studies. The increasing semantic interpretability of the visualized perturbations suggests that the adversarial examples capture the common features of models on the natural image manifold, while the loss of effectiveness on adversarially trained models indicates that the scaling comes from the shareable feature space across diverse models [90].

## 2. Related Work

### 2.1. Black-Box Attacks

Deep learning models are widely recognized for their vulnerability to adversarial attacks [33, 76]. Extensive research has documented this susceptibility, particularly in image classification contexts [4, 10], under two principal settings: white-box and black-box attacks. In the white-box setting, the adversary has complete access to the target model [63]. Conversely, in the black-box setting, such information is obscured from the attacker. With limited access to the target model, black-box attacks typically either construct queries and rely on feedback from the model [26, 42] or leverage the transferability of predefined surrogate models [58]. Query-based attacks often suffer from high time complexity and substantial computational costs, making transfer-based methods more practical and cost-effective for generating adversarial examples, as they do not necessitate direct interaction with target models during the training phase.

Within the realm of transfer-based attacks, existing methods can generally be categorized into three types: input transformation, gradient-based optimization, and ensemble attacks. Input transformation methods employ data augmentation techniques before feeding inputs into models, such as resizing and padding [92], translations [25], or transforming them into frequency domain [61]. Gradient-based methods concentrate on designing optimization algorithms to improve transferability, incorporating strategies such as momentum optimization [24, 54], scheduled step sizes [31], and gradient variance reduction [85].

### 2.2. Ensemble Attacks

Inspired by model ensemble techniques in machine learning [21, 32, 90], researchers have developed sophisticated adversarial attack strategies utilizing sets of surrogate models. In forming an ensemble paradigm, practitioners often average over losses [24], predictions [58], or logits [24]. Additionally, advanced ensemble algorithms have been proposed to enhance adversarial transferability [11, 13, 53, 95]. However, these approaches tend to treat model ensemble as a mere technique for improving transferability without delving into the underlying principles.

Prior studies [39] indicate that increasing the number of classifiers in adversarial attacks can effectively reduce the

upper bound of generalization error in Empirical Risk Minimization (ERM). Recent research [97] has theoretically defined transferability error and sought to minimize it through model ensemble. Nonetheless, while an upper bound is given, they do not really scale up in practice and have to train neural networks from scratch to meet the assumption of sufficient diversity among ensemble models [57].

### 2.3. Scaling Laws

In recent years, the concept of scaling laws has gained significant attention. These laws describe the relationship between model size – measured in terms of parameters, data, or training FLOPs – and generalization ability, typically reflected in evaluation loss [46]. Subsequent studies have expanded on scaling laws from various perspectives, including image classification [5, 36], language modeling [72] and mixture of experts (MoE) models [75], highlighting the fundamental nature of this empirical relationship.

In the domain of adversarial attack research, recent work has attempted to derive scaling laws for adversarially trained defense models on CIFAR-10 [8, 48]. However, the broader concept of scaling remains underexplored. While some preliminary observations on the effect of enlarging model ensemble can be found in prior studies [3, 97], these effects have not been systematically analyzed. In this paper, however, we focus on the empirical scaling laws within model ensembles, and verify it through extensive experiments on open-source pretrained models. Motivated by this perspective, we unveil vulnerabilities within commercial LLMs by targeting their vision encoders.

## 3. Backgrounds

In this section, we propose necessary backgrounds including problem formulation and algorithms.

### 3.1. Problem Formulation

In this work, we focus on the challenging targeted attack setting. Let  $\mathcal{F}$  denote the set of all image classifiers. Given a natural image  $\mathbf{x}_{\text{nat}}$  and target class  $\mathbf{y}$ , the goal of targeted transfer-based attacks is to craft an adversarial example  $\mathbf{x}$  that is misclassified to  $\mathbf{y}$  by all models in  $\mathcal{F}$ . It can be formulated as a constrained optimization problem:

$$\min_{\mathbf{x}} \mathbb{E}_{f \in \mathcal{F}} [\mathcal{L}(f(\mathbf{x}), \mathbf{y})], \text{ s.t. } \|\mathbf{x} - \mathbf{x}_{\text{nat}}\|_{\infty} \leq \epsilon, \quad (1)$$

where  $\mathcal{L}$  is the loss function (e.g., cross-entropy loss), and we consider adversarial perturbations in  $\ell_{\infty}$  norm.

Generally, we take a limited set of “training” classifiers  $\mathcal{F}_T := \{f_i\}_{i=1}^T \subset \mathcal{F}$  as model ensemble to approximate problem (1) and therefore the optimization objective becomes:

$$\min_{\mathbf{x}} \frac{1}{T} \sum_{i=1}^T \mathcal{L}(f_i(\mathbf{x}), \mathbf{y}), \text{ s.t. } \|\mathbf{x} - \mathbf{x}_{\text{nat}}\|_{\infty} \leq \epsilon, \quad (2)$$

where  $T = |\mathcal{F}_T|$  is the cardinality of model ensemble.

### 3.2. Prerequisite Algorithms

Researchers have been developing sophisticated algorithms for ensemble attacks, and we select SOTA algorithms from them to conduct our experiments.

**Momentum Iterative Fast Gradient Sign Method.** MI-FGSM [24] stabilizes the gradient updating directions by integrating a momentum term into the iterative process, which generates the momentum by

$$\mathbf{g}_{t+1} = \mu \cdot \mathbf{g}_t + \frac{\nabla_{\mathbf{x}} \mathcal{L}(\mathbf{x}_t, \mathbf{y})}{\|\nabla_{\mathbf{x}} \mathcal{L}(\mathbf{x}_t, \mathbf{y})\|_1}, \quad (3)$$

and updates  $\mathbf{x}$  by

$$\mathbf{x}_{t+1} = \mathbf{x}_t + \alpha \cdot \text{sign}(\mathbf{g}_{t+1}). \quad (4)$$

**Common Weakness Method.** The common weakness attack (CWA) [13] seeks to identify shared vulnerabilities across surrogate models by encouraging flatter loss landscapes and closer proximity between local optima of these models, which is minimizing the second-order Taylor series

$$\frac{1}{T} \sum_{i=1}^T \left[ \mathcal{L}(f_i(\mathbf{p}_i, \mathbf{y}) + \frac{1}{2}(\mathbf{x} - \mathbf{p}_i)^{\top} H_i(\mathbf{x} - \mathbf{p}_i) \right], \quad (5)$$

where  $\mathbf{p}_i$  denotes the closest optimum of model  $f_i$  to  $\mathbf{x}$  and  $H_i$  is the Hessian matrix at  $\mathbf{p}_i$ .

**CWA enables the scaling laws.** Since the gradients of normally trained models commonly lack semantics and have random directions, naive ensemble methods that directly average these gradients lead to strong gradient conflicts, significantly impacting optimization. As shown in Fig. 2, as the number of models increases, gradient conflicts among other optimizers (MI-FGSM [24] here) be-

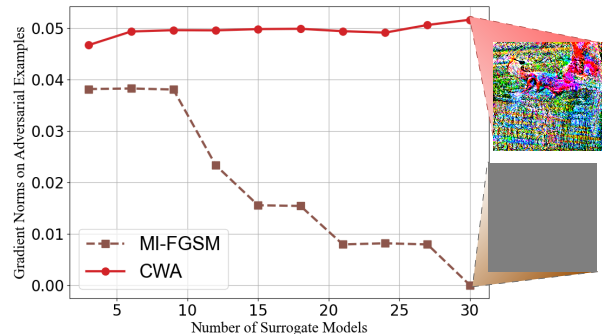


Figure 2. Comparisons between CWA and MI-FGSM methods. We measure the averaged gradient magnitudes on  $\mathbf{x}$  after 10 steps of iteration, and record the results across  $T$  from 1 to 30. On the right side there are the visualizations of gradients of  $T = 30$ .

ASR(%)	Target: Car		Target: Ship	
	MI-CWA	SSA-CWA	MI-CWA	SSA-CWA
Swin-v2	0.44	<b>0.65</b>	0.36	<b>0.62</b>
ConvNeXt	0.52	<b>0.58</b>	0.53	<b>0.62</b>
ResNet50	0.69	<b>0.79</b>	0.66	<b>0.77</b>

Table 1. Comparison of ASR between SSA and MI algorithms. We follow the experiment settings in Sec. 4.2, and measure the ASR on 2 target classes and 3 black-box models.

come more severe, eventually reducing the ensemble gradient to zero and resulting in complete optimization stagnation. CWA not only fully avoids this issue but also promotes gradient alignment, causing the gradient magnitude to increase as the number of models grows. This demonstrates that CWA achieves a significantly higher information utilization rate than other optimizers, avoiding gradient conflict, and thus enabling the scaling laws.

**Spectrum Simulation Method.** The spectrum simulation attack (SSA) [61] enhances adversarial transferability by applying a spectrum transformation  $\mathcal{T}$  to the input data and calculate gradients with respect to  $\mathcal{T}(\mathbf{x})$  instead of  $\mathbf{x}$ . As the variable of differentiation changes, SSA cannot combine with MI, but both of them can combine with CWA by changing their optimization objectives. As shown in Table 1, SSA achieves the success rate of 10% higher compared with MI algorithm, demonstrating its effectiveness of generating diverse spectrum saliency maps [61]. This encourages us to select it as key algorithm in our experiments.

## 4. Scaling Laws for Adversarial Attacks

In this section, we bring our key findings on scaling laws for black-box adversarial attacks. Sec. 4.1 introduces fundamental concepts and theorems that give us motivations for the study of scaling laws. Sec. 4.2 contains our experiment settings and derivations of our empirical scaling laws. Sec. 4.3 demonstrates the results when we take vision language models as black-box models.

### 4.1. Motivations

Firstly, we observe that in most practical scenarios,  $\mathbf{x}_{\text{nat}}$  and  $\mathbf{y}$  are predefined and fixed. Consequently, Eq. (1) and Eq. (2) can be considered as functions of variable  $\mathbf{x}$  only.

**Definition 1.** Define  $\mathbf{x}^*$  and  $\hat{\mathbf{x}}$  to be the minimizer of Eq. (1) and Eq. (2) respectively, which can be written as

$$\begin{aligned} \mathbf{x}^* &= \arg \min_{\mathbf{x}} \mathbb{E}_{f \in \mathcal{F}} [\mathcal{L}(f(\mathbf{x}), \mathbf{y})], \\ \hat{\mathbf{x}} &= \arg \min_{\mathbf{x}} \frac{1}{T} \sum_{i=1}^T \mathcal{L}(f_i(\mathbf{x}), \mathbf{y}), \end{aligned} \quad (6)$$

with the same  $\ell_\infty$  norm constraints given in Eq. (1) and (2).

**Definition 2.** Define  $\mathbb{L}(\cdot)$  as the population loss in Eq. (1), and  $\mathbb{L}(f_i(\cdot))$  as the loss on one surrogate model  $f_i$ :

$$\begin{aligned} \mathbb{L}(\mathbf{x}) &= \mathbb{E}_{f \in \mathcal{F}} [\mathcal{L}(f(\mathbf{x}), \mathbf{y})], \\ \mathbb{L}(f_i(\mathbf{x})) &= \mathcal{L}(f_i(\mathbf{x}), \mathbf{y}). \end{aligned} \quad (7)$$

These definitions are used to simplify our notations and better demonstrate our proofs. Then we bring our key observations that are shown in the following theorem.

**Theorem 1.** Suppose that model ensemble  $\{f_i\}_{i=1}^T$  is i.i.d. sampled from some distribution on  $\mathcal{F}$ , and  $\hat{\mathbf{x}}$  goes to  $\mathbf{x}^*$  as  $T \rightarrow \infty$ . Denote  $\xrightarrow{d}$  as convergence in distribution, and  $\text{Cov}$  as the covariance matrix. Then we have the following asymptotic bound as  $T \rightarrow \infty$ :

$$\begin{aligned} \sqrt{T}(\hat{\mathbf{x}} - \mathbf{x}^*) &\xrightarrow{d} \mathcal{N}(0, (\nabla^2 \mathbb{L}(\mathbf{x}^*))^{-1} \text{Cov}(\mathbb{L}(f_i)) (\nabla^2 \mathbb{L}(\mathbf{x}^*))^{-1}), \\ T(\mathbb{L}(\hat{\mathbf{x}}) - \mathbb{L}(\mathbf{x}^*)) &\xrightarrow{d} \frac{1}{2} \|S\|_2^2, \text{ with} \\ S &\sim \mathcal{N}(0, (\nabla^2 \mathbb{L}(\mathbf{x}^*))^{1/2} \text{Cov}(\mathbb{L}(f_i)) (\nabla^2 \mathbb{L}(\mathbf{x}^*))^{1/2}). \end{aligned} \quad (8)$$

Proof of Theorem 1 can be found in Appendix A.

**Remark 1.** Theorem 1 suggests that the adversarial examples converge in  $\mathcal{O}(\frac{1}{\sqrt{T}})$ , while the difference between population loss and empirical loss converges in  $\mathcal{O}(\frac{1}{T})$ .

When we replace  $\mathcal{L}$  with cross-entropy loss in Theorem 1, we get Theorem 2 by some simple derivations.

**Theorem 2.** Following the notation and assumptions in Theorem 1, when using negative likelihood loss (cross entropy), we have:

$$\begin{aligned} \sqrt{T}(\hat{\mathbf{x}} - \mathbf{x}^*) &\xrightarrow{d} \mathcal{N}(0, (\nabla^2 \mathbb{L}(\mathbf{x}^*))^{-1}), \\ T(\mathbb{L}(\hat{\mathbf{x}}) - \mathbb{L}(\mathbf{x}^*)) &\xrightarrow{d} \frac{1}{2} \|\mathcal{N}(0, \mathbf{I})\|_2^2. \end{aligned} \quad (9)$$

**Remark 2.** The above holds since  $\text{Cov}(\mathbb{L}(f_i(\mathbf{x}^*))) = \nabla^2 \mathbb{L}(\mathbf{x}^*)$  for cross entropy loss. Thus we have  $2T(\mathbb{L}(\hat{\mathbf{x}}) - \mathbb{L}(\mathbf{x}^*)) \xrightarrow{d} \chi^2(D)$  where  $D$  is the dimension of the input images, which means  $\mathbb{L}(\hat{\mathbf{x}}) - \mathbb{L}(\mathbf{x}^*)$  converges in  $\mathcal{O}(\frac{D}{2T})$ .

Theorem 2 gives us motivations on further exploring the affects of ensemble cardinality  $T$  as empirical loss converges with a factor of  $T$ . This leads us to recovering the scaling laws on black-box adversarial attacks.

### 4.2. Scaling Laws on Image Classifiers

Before demonstrating scaling laws, we first introduce our experiment settings and hyperparameters.

**Surrogate Models.** To ensure the transferability and diversity of models, we select 64 models, with 62 pretrained



models from Torchvision [64] and Timm [87] with different hyperparameters, architectures, and training datasets – Alexnet [49], Densenet [38], Efficientnet [79], Googlenet [77], Inception-V3 [78], Maxvit [84], Mnasnet [80], Mobilenet [37], Regnet [96], Resnet [35], Shufflenet [99], Squeezenet [41], Vgg [73], ViT [28], WideResnet [98], Beit [7], Ghostnet [34], Deit [81], LCnet [17, 88], Repvgg [22], Dpn [14], Mit [93], Bit [47], CvT [91], and 2 adversarially trained models available on Robustbench - FGSMAT [50] with Inception-V3, Ensemble AT (EnsAT) [83] with Inception-ResNet-V2. The full list of our surrogate models can be found in Appendix B.

**Black-box Models.** We carefully choose models that are both widely known and are different from training ensembles in architecture and hyperparameters. We select 7 models as our target models, including Swin-Transformers [59], ConvNeXt [60], and ResNeXt [94].

**Dataset.** Following previous works [45], we randomly take 100 images from the NIPS17 dataset \*. All images are resized into  $224 \times 224$ . We select 5 categories as target labels, including *cat*, *car*, *ship*, *deer* and *bird*.

**Hyperparameters.** We set the perturbation budget  $\epsilon = 8/255$  under  $\ell_\infty$  norm. We take 40 iteration steps of SSA-CWA, while other hyper-parameter settings are the same as in [13]. We set the loss function  $\mathcal{L}$  to be cross entropy loss between the output logit  $f(x)$  and the label  $y$ .

**Experiment Results.** The results of ensemble attacks are shown in Fig. 3. From our observations, we empirically derive the scaling laws between the attack success rate (ASR) and ensemble cardinality  $T$  as follows:

$$\text{ASR} = \alpha \log T + C. \quad (10)$$

It can be explained by the following points:

- $C$  is influenced by various factors, such as hyperparameters, model architectures, and adversarial targets, and therefore takes different values under different conditions.
- For a fixed adversarial target,  $\alpha$  depends solely on the model architecture. Models with the same architecture share the same  $\alpha$ , regardless of hyperparameter settings.
- When  $T$  is small, the measured ASR exhibits large variance due to different model selections, suggesting that our scaling laws tend to be a statistical result.
- ASR acts as a good representation of the empirical loss  $\mathbb{L}$ , with low evaluation loss resulting in high ASR generally. In fact it can be observed from Fig. 3 that there exists strong symmetry between  $\mathbb{L}$  and ASR.
- The scaling laws become less useful as the ASR approaches 1, since ASR no longer reflects  $\mathbb{L}$  at that point. This indicates that our observations hold only when the success rate is below the converging threshold.

\*<https://www.kaggle.com/competitions/nips-2017-non-targeted-adversarial-attack>

Our experiment results clearly show that transferability of adversarial images exists, independent of specific test models or adversarial targets. It is important to note that both our training and evaluation models are open-sourced and pretrained on ImageNet [20], which means they do not strictly satisfy the i.i.d. assumption discussed in Sec. 4.1. Therefore, the theorems derived in Sec. 4.1 should be viewed as a sign of convergence and are not directly related with the empirical result measured by our experiments. Another key improvement observed from our scaling laws is that the evaluation loss  $\mathbb{L}$  decreases exponentially with the ensemble cardinality  $T$ , which is much tighter compared to bounds derived in previous works [39, 97].

### 4.3. Scaling Laws on Vision Language Models

Vision language models (VLMs) have demonstrated impressive abilities in image understanding, describing and reasoning [9, 70, 82]. In this part we show that our scaling laws persist in these VLMs.

**Black-box Models.** We still leverage the adversarial examples generated against traditional image classifiers and select 3 popular VLMs – LLaVA-v1.5-7b [56], DeepSeek-VL-7b [19], and Phi-3-vision [1] as test models.

**Evaluation Metrics.** As VLMs output prompts rather than logits, we adopt the definition of ASR from MultiTrust [100], which leverages GPT4 for determining whether the targeted object is stated in the description. In addition to assessing the correctness of the image classification, it introduces prompts to evaluate the degree of distortion in the crafted image. If GPT determines that the image is highly corrupted, the attack is considered unsuccessful, even if the test model misclassifies the image. This metric ensures our judgments of successful attacks are of high quality.

**Experiment Results.** From the results presented in Fig. 4, several key observations can be drawn:

- All models exhibit a similar value of  $C$ , indicating that they are all highly robust to attack patterns when the ensemble cardinality  $T$  is small.
- $\alpha$  varies significantly across models, revealing the considerable differences in robustness between VLMs.
- Since VLMs are trained on multimodal data, different adversarial targets significantly influence the attack success rates. This variability may stem from the inherent characteristics of the target labels, as naturally some labels (such as “deer”) are less representative compared to labels like “cat”. This phenomenon, often referred to as class imbalance, has been discussed in prior studies [44].

When compared to image classifiers, VLMs demonstrate superior robustness across all chosen adversarial targets. This supports the general opinion that multimodal training leads to more robust representations [40], enabling the model to focus more on the essential features of the image rather than specific attack patterns. Furthermore, in con-

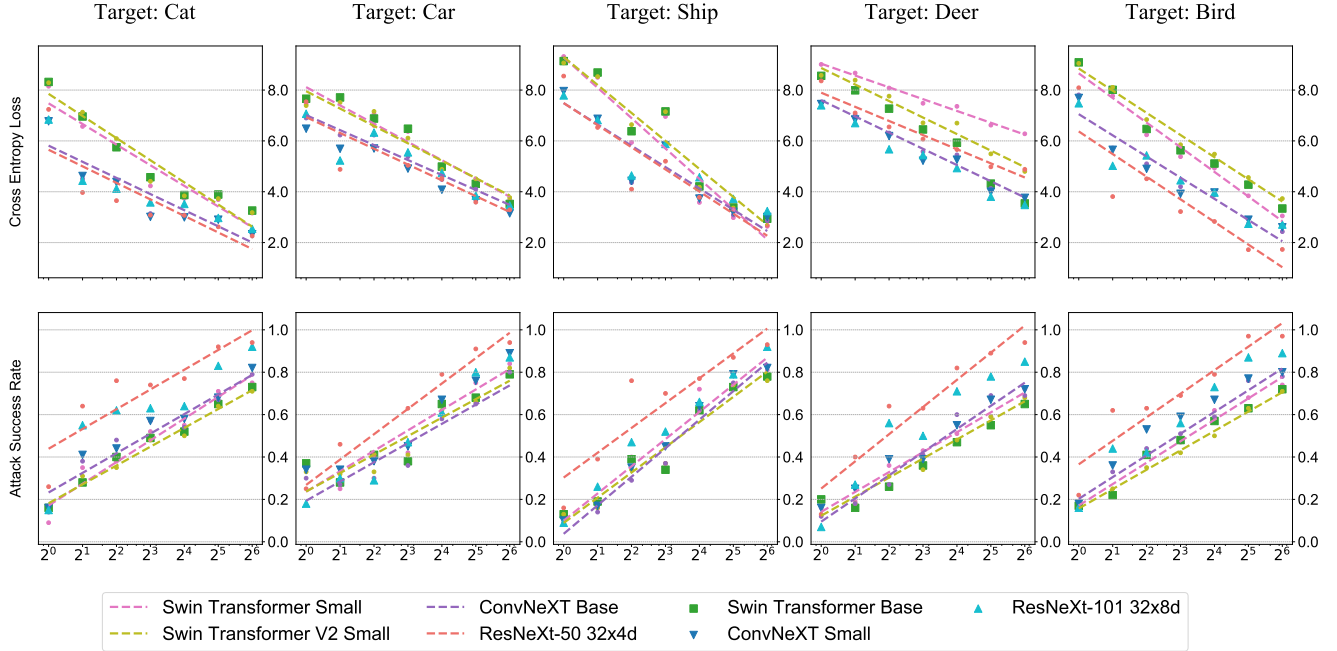


Figure 3. Scaling Laws over model ensemble in a black-box setting. We plot the x-axis on a base-2 logarithmic scale, and we measure both the attack success rate (ASR) and averaged cross entropy loss of test models. The cardinality of the model ensembles is varied from  $2^0$  to  $2^6$ , with models randomly selected for each ensemble. We fit the results of 4 test models by lines for better demonstration.

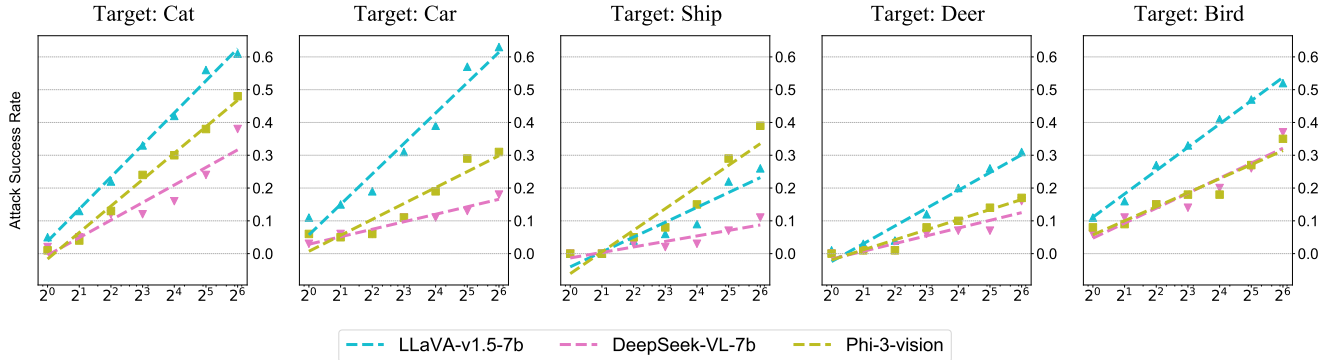


Figure 4. Scaling Laws on VLMs. We measure the ASR of test VLMs and fit the results with lines. Note that scaling laws still exists except for the fact that results vary largely between models and targets.

trast to traditional views that scaling model parameters results in increased robustness, we find that among the three target models, *Phi-3-vision* exhibits the highest robustness. This observation suggests that the scaling laws derived in [8] may not be directly applicable to multimodal models.

## 5. Extending Scaling Laws to Vision Encoders

In this section we extend our findings of scaling laws from image classifiers to multimodal foundation models such as CLIPs. Sec. 5.1 shows the extension of Eq. (2) to image embeddings, while Sec. 5.2 demonstrates high success rates over commercial multimodal large language models

(MLLMs) under our framework.

### 5.1. Attacking Image Embeddings

Contrastive Language-Image Pretraining (CLIP) is a popular self-supervised framework that can pretrain large-scale language-vision models on web-scale text-image pairs via contrastive learning [71]. Compared to image classifiers that are normally trained on image classification datasets, CLIPs have demonstrated superior zero shot generalization abilities in multimodal downstream tasks [51, 67].

Based on the generalization ability of CLIP models, previous works have utilized them as surrogate models in

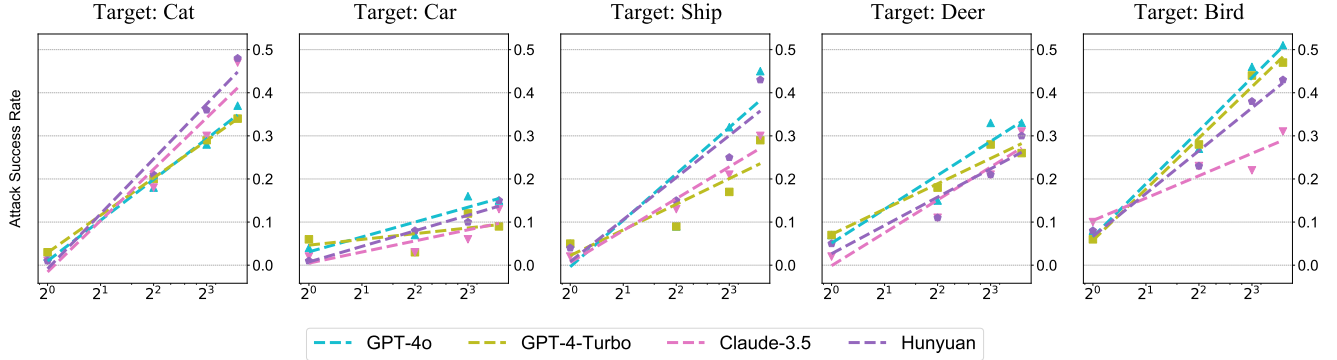


Figure 5. Demonstrations of scaling laws when we use CLIPs as surrogate models under  $\epsilon = 8/255$ . We take ASR measured by Metric 1 to ensure our results are of high confidence.

model ensembles [3, 27, 30]. In fact, the targeted attack framework described in Eq. (2) can be easily extended by replacing the loss function  $\mathcal{L}$  with the similarity measure  $\text{sim}(\cdot)$  from CLIP (usually cosine embedding loss in practice), and by substituting the image classifiers  $f$  with CLIP’s image encoders  $f^I$ . This modification leads to the following optimization objective:

$$\min_{\mathbf{x}} \frac{1}{T} \sum_{j=1}^T \text{sim}(f_j^I(\mathbf{x}), f_j^I(\mathbf{x}_{\text{tar}})), \text{ s.t. } \|\mathbf{x} - \mathbf{x}_{\text{nat}}\|_{\infty} \leq \epsilon. \quad (11)$$

Note that besides an empirical loss function, Eq. (11) can be also explained as minimizing the distance between the embeddings of the adversarial examples and the target images on a low-dimension embedding manifold.

## 5.2. Experiments and Evaluations

We first introduce our settings for attacking pretrained CLIP models and MLLMs used for our evaluation.

**Surrogate Models.** We select 12 pretrained open-source CLIP models via OpenCLIP [15]. In contrast to previous works that typically use fewer than 4 surrogate models, our ensemble choice is sufficient to yield robust results. These CLIP models vary in architecture, hyperparameters, input image sizes, and even training datasets.

**Black-box Target Models.** We choose 5 commercial MLLMs from the MultiTrust leaderboard with high robustness as our target black-box models: GPT-4o, GPT-4-turbo [66], Claude-3.5-sonnet<sup>†</sup>, Hunyuan [75], and Qwen [6].

**Hyperparameters.** To demonstrate the scaling laws, we set  $\epsilon = 8/255$ . For practical applications, we follow the common settings in [27, 62] and set  $\epsilon = 16/255$ . All other experiment settings are consistent with those in Sec. 4.

**Evaluation Metrics.** We employ two types of evaluation metrics in this study. The first metric is the same as in

Sec. 4.3. The second metric focuses on the features of adversarial examples, whose goal is to evaluate the insertion of features within adversarial targets into these examples. It requires the test model to generate a description and asks GPT whether the description mentions the adversarial target. Both metrics take ASR as the final score, which we refer to as **Metric 1** and **Metric 2** in the following sections for simplicity. Test prompts can be found in Appendix C.

**Experiment Results.** Fig. 5 presents the experiment results on the test models under Metric 1. These results reveal that scaling laws continue to hold when using CLIP models as surrogate models. This outcome seems natural as image features are still correctly learned within the vision encoders. Our method achieves success rates of over 30% on most adversarial targets under Metric 1, indicating that more than 1/3 of the original images are transformed into high-quality adversarial examples with minimal noise, which demonstrates the efficiency of our method.

We also conduct extensive experiments using Metric 2. Table 2 shows our attack success rates across some of the test LLMs (results of other models can be found in Appendix D). Remarkably, under  $\epsilon = 16/255$ , our CLIP ensemble achieves over 90% success on the GPT series and more than 60% on other commercial LLMs. These results highlight the inherent vulnerabilities of commercial LLMs and underscore the need for the development of more robust and trustworthy multimodal foundation models.

## 6. Further Studies

In this section, we conduct further studies of our scaling laws derived in the past sections. We attempt to explain the existence of scaling laws from two perspectives: first through the visualization of adversarial perturbations, and second by showing that scaling laws do not hold in adversarially trained models.

<sup>†</sup><https://www.anthropic.com/news/claude-3-family>

ASR(%)	Target: Cat		Target: Car		Target: Ship		Target: Deer		Target: Bird	
$\epsilon$ ( $\ell_\infty$ norm)	8/255	16/255	8/255	16/255	8/255	16/255	8/255	16/255	8/255	16/255
GPT-4o	0.58	<b>0.99</b>	0.22	<b>0.52</b>	0.57	<b>0.91</b>	0.40	<b>0.89</b>	0.56	<b>0.97</b>
GPT-4-Turbo	0.68	<b>0.99</b>	0.23	<b>0.55</b>	0.59	<b>0.92</b>	0.38	<b>0.86</b>	0.61	<b>0.97</b>
Claude-3.5	0.56	<b>0.91</b>	0.18	<b>0.42</b>	0.41	<b>0.79</b>	0.37	<b>0.74</b>	0.38	<b>0.80</b>

Table 2. ASR under Metric 2 measured across different settings of  $\epsilon$ . Remarkably, combined with our methods, most adversarial examples are considered to contain the targets’ features by MLLMs given  $\epsilon = 16/255$ .

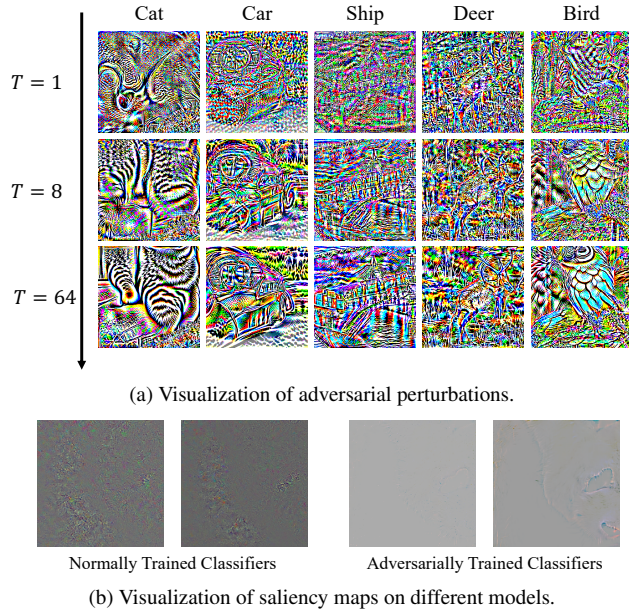


Figure 6. Visualization for analysis. (a) It demonstrates the trend of the increasing semantic interpretability of adversarial perturbations over different target objects. (b) It shows the saliency maps of normal image classifiers and adversarially trained models, measured by the first step of the gradient descent iterations.

## 6.1. Visualizations of adversarial perturbations

As shown in Fig. 6a, the semantic meaning of our adversarial perturbations also increases as the cardinality of the model ensemble grows. This suggests that the attack success rates are closely related to the interpretability of the perturbations, aligning with human observations and preferences [18]. Since the ultimate goal of adversarial attacks is to generate high-quality adversarial examples, it is preferable to have interpretable perturbations, as this reinforces the idea that the scaling effectively helps learn common features, rather than merely converging to local optima.

As people traditionally believe images lie on a low dimensional manifold of desirable properties [29], this interpretability of adversarial examples can be also understood within the feature space of images, where human-designed attack algorithms aim to eliminate the non-robust features of images and shift the image towards the robust features of

the target class [43]. From this perspective, our approach of enlarging model ensembles seeks to provide more information about the manifold itself, offering more accurate representations of the image features.

When we enlarge  $\epsilon$  from 8/255 to 16/255 or even larger, the affect of the natural image goes down to 0, and the adversarial attack task degenerates to an image generation task. We claim that our method of scaling model ensemble still remains good performance under the degenerated image generation task, where the visualized results are shown in Appendix E.

## 6.2. Limitations of Scaling Laws

Though we have derived scaling laws from normal image classifiers, the results on adversarially trained models disapprove the fact of scaling in our experiments. The experiment settings and results can be found in Appendix F, where we demonstrate that enlarging the cardinality of model ensemble do not actually increase transfer attack success rates over all these adversarial defense models. By visualization of saliency maps between adversarially trained models and normal image classifiers in Fig. 6b, we observe that they have a completely different focus when performing gradient descent on  $x$ . The result supports that scaling laws exist only when the target models and surrogate models follow the same distribution (i.e., are independently sampled from an identical model set), which corroborates the i.i.d. assumption in Theorem 1.

## 7. Conclusion

In this work, we investigate the scaling laws for black-box adversarial attacks. Based on state-of-the-art transfer attack algorithms, we first provide theoretical motivations on the convergence of adversarial examples and training loss, and then propose the scaling laws empirically by our observations that the attack success rate (ASR) and the loss are converging in an exponential manner. We conduct extensive experiments over both image classifiers and modern vision language models (VLMs) to state our scaling laws are robust enough under different scenarios. Leveraging our insights of scaling laws, we emphasize possible practical applications by attacking commercial Multimodal Large Language Models (MLLMs) targeting on an ensemble of CLIP



vision encoders. We eventually analyze the reasons of the scaling laws for adversarial attack, from the perspectives of perturbation visualization and evaluation on adversarially trained models. We believe the findings in this work can help deepen the understanding of the weaknesses of vision models regarding adversarial robustness in a black-box context, ultimately contributing to the development of more robust and trustworthy multimodal foundation models.

## References

- [1] Marah Abdin, Jyoti Aneja, Hany Awadalla, Ahmed Awadallah, Ammar Ahmad Awan, Nguyen Bach, Amit Bahree, Arash Bakhtiari, Jianmin Bao, Harkirat Behl, Alon Benhaim, Misha Bilenko, Johan Bjorck, Sébastien Bubeck, Martin Cai, Qin Cai, Vishrav Chaudhary, Dong Chen, Dongdong Chen, Weizhu Chen, Yen-Chun Chen, Yi-Ling Chen, Hao Cheng, Parul Chopra, Xiyang Dai, Matthew Dixon, Ronen Eldan, Victor Fragoso, Jianfeng Gao, Mei Gao, Min Gao, Amit Garg, Allie Del Giorno, Abhishek Goswami, Suriya Gunasekar, Emman Haider, Junheng Hao, Russell J. Hewett, Wenxiang Hu, Jamie Huynh, Dan Iter, Sam Ade Jacobs, Mojan Javaheripi, Xin Jin, Nikos Karampatziakis, Piero Kauffmann, Mahoud Khademi, Dongwoo Kim, Young Jin Kim, Lev Kurilenko, James R. Lee, Yin Tat Lee, Yanzhi Li, Yunsheng Li, Chen Liang, Lars Liden, Xihui Lin, Zeqi Lin, Ce Liu, Liyuan Liu, Mengchen Liu, Weishung Liu, Xiaodong Liu, Chong Luo, Piyush Madan, Ali Mahmoudzadeh, David Majercak, Matt Mazzola, Caio César Teodoro Mendes, Arindam Mitra, Hardik Modi, Anh Nguyen, Brandon Norick, Barun Patra, Daniel Perez-Becker, Thomas Portet, Reid Pryzant, Heyang Qin, Marko Radmilac, Liliang Ren, Gustavo de Rosa, Corby Rosset, Sambudha Roy, Olatunji Ruwase, Olli Saarikivi, Amin Saied, Adil Salim, Michael Santacroce, Shital Shah, Ning Shang, Hiteshi Sharma, Yelong Shen, Swadheen Shukla, Xia Song, Masahiro Tanaka, Andrea Tupini, Praneetha Vaddamanu, Chunyu Wang, Guanhua Wang, Lijuan Wang, Shuohang Wang, Xin Wang, Yu Wang, Rachel Ward, Wen Wen, Philipp Witte, Haiping Wu, Xiaoxia Wu, Michael Wyatt, Bin Xiao, Can Xu, Jiahang Xu, Weijian Xu, Jilong Xue, Sonali Yadav, Fan Yang, Jianwei Yang, Yifan Yang, Ziyi Yang, Donghan Yu, Lu Yuan, Chenruidong Zhang, Cyril Zhang, Jianwen Zhang, Li Lina Zhang, Yi Zhang, Yue Zhang, Yunan Zhang, and Xiren Zhou. Phi-3 technical report: A highly capable language model locally on your phone, 2024. [5](#)
- [2] Sajjad Amini, Mohammadreza Teymorianfard, Shiqing Ma, and Amir Houmansadr. Meansparse: Post-training robustness enhancement through mean-centered feature sparsification, 2024. [17](#)
- [3] Anonymous. TUAP: Targeted universal adversarial perturbations for CLIP. In *Submitted to The Thirteenth International Conference on Learning Representations*, 2024. under review. [3](#), [7](#), [15](#)
- [4] Anish Athalye, Nicholas Carlini, and David Wagner. Obfuscated gradients give a false sense of security: Circumventing defenses to adversarial examples. In *International conference on machine learning*, pages 274–283. PMLR, 2018. [2](#)
- [5] Yasaman Bahri, Ethan Dyer, Jared Kaplan, Jaehoon Lee, and Utkarsh Sharma. Explaining neural scaling laws. *Proceedings of the National Academy of Sciences*, 121(27): e2311878121, 2024. [3](#)
- [6] Jinze Bai, Shuai Bai, Yunfei Chu, Zeyu Cui, Kai Dang, Xiaodong Deng, Yang Fan, Wenbin Ge, Yu Han, Fei Huang, Binyuan Hui, Luo Ji, Mei Li, Junyang Lin, Runji Lin, Dayiheng Liu, Gao Liu, Chengqiang Lu, Keming Lu, Jianxin Ma, Rui Men, Xingzhang Ren, Xuancheng Ren, Chuanqi Tan, Sinan Tan, Jianhong Tu, Peng Wang, Shijie Wang, Wei Wang, Shengguang Wu, Benfeng Xu, Jin Xu, An Yang, Hao Yang, Jian Yang, Shusheng Yang, Yang Yao, Bowen Yu, Hongyi Yuan, Zheng Yuan, Jianwei Zhang, Xingxuan Zhang, Yichang Zhang, Zhenru Zhang, Chang Zhou, Jingren Zhou, Xiaohuan Zhou, and Tianhang Zhu. Qwen technical report, 2023. [7](#), [15](#)
- [7] Hangbo Bao, Li Dong, Songhao Piao, and Furu Wei. Beit: Bert pre-training of image transformers. *arXiv preprint arXiv:2106.08254*, 2021. [5](#)
- [8] Brian R. Bartoldson, James Diffenderfer, Konstantinos Parasyris, and Bhavya Kailkhura. Adversarial robustness limits via scaling-law and human-alignment studies, 2024. [3](#), [6](#)
- [9] Tom B Brown. Language models are few-shot learners. *arXiv preprint arXiv:2005.14165*, 2020. [5](#)
- [10] Nicholas Carlini and David Wagner. Towards evaluating the robustness of neural networks. In *2017 IEEE Symposium on Security and Privacy (SP)*, pages 39–57. Ieee, 2017. [2](#)
- [11] Bin Chen, Jiali Yin, Shukai Chen, Bohao Chen, and Ximeng Liu. An adaptive model ensemble adversarial attack for boosting adversarial transferability. In *Proceedings of the IEEE/CVF International Conference on Computer Vision*, pages 4489–4498, 2023. [2](#)
- [12] Erh-Chung Chen and Che-Rung Lee. Data filtering for efficient adversarial training. *Pattern Recognition*, 151: 110394, 2024. [17](#)
- [13] Huanran Chen, Yichi Zhang, Yinpeng Dong, Xiao Yang, Hang Su, and Jun Zhu. Rethinking model ensemble in transfer-based adversarial attacks. *arXiv preprint arXiv:2303.09105*, 2023. [2](#), [3](#), [5](#), [15](#)
- [14] Yunpeng Chen, Jianan Li, Huaxin Xiao, Xiaojie Jin, Shuicheng Yan, and Jiashi Feng. Dual path networks. *Advances in neural information processing systems*, 30, 2017. [5](#)
- [15] Mehdi Cherti, Romain Beaumont, Ross Wightman, Mitchell Wortsman, Gabriel Ilharco, Cade Gordon, Christoph Schuhmann, Ludwig Schmidt, and Jenia Jitsev. Reproducible scaling laws for contrastive language-image learning. In *Proceedings of the IEEE/CVF Conference on Computer Vision and Pattern Recognition*, pages 2818–2829, 2023. [7](#), [15](#)
- [16] Francesco Croce, Maksym Andriushchenko, Vikash Sehwag, Edoardo DeBenedetti, Nicolas Flammarion, Mung Chiang, Prateek Mittal, and Matthias Hein. Robustbench: a standardized adversarial robustness benchmark, 2021. [16](#)

- [17] Cheng Cui, Tingquan Gao, Shengyu Wei, Yuning Du, Ruoyu Guo, Shuilong Dong, Bin Lu, Ying Zhou, Xueying Lv, Qiwen Liu, et al. Pp-lcnet: A lightweight cpu convolutional neural network. *arXiv preprint arXiv:2109.15099*, 2021. 5
- [18] Zheng Dai and David Gifford. Fundamental limits on the robustness of image classifiers. In *The Eleventh International Conference on Learning Representations*, 2022. 8
- [19] DeepSeek-AI. Deepseek llm: Scaling open-source language models with longtermism. *arXiv preprint arXiv:2401.02954*, 2024. 5, 15
- [20] J. Deng, W. Dong, R. Socher, L.-J. Li, K. Li, and L. Fei-Fei. ImageNet: A Large-Scale Hierarchical Image Database. In *CVPR09*, 2009. 5
- [21] Thomas G Dietterich. Ensemble methods in machine learning. In *International workshop on multiple classifier systems*, pages 1–15. Springer, 2000. 2
- [22] Xiaohan Ding, Xiangyu Zhang, Ningning Ma, Jungong Han, Guiguang Ding, and Jian Sun. Repvgg: Making vgg-style convnets great again. In *Proceedings of the IEEE/CVF conference on computer vision and pattern recognition*, pages 13733–13742, 2021. 5
- [23] Yinpeng Dong, Hang Su, Jun Zhu, and Fan Bao. Towards interpretable deep neural networks by leveraging adversarial examples. *arXiv preprint arXiv:1708.05493*, 2017. 1
- [24] Yinpeng Dong, Fangzhou Liao, Tianyu Pang, Hang Su, Jun Zhu, Xiaolin Hu, and Jianguo Li. Boosting adversarial attacks with momentum. In *Proceedings of the IEEE conference on computer vision and pattern recognition*, pages 9185–9193, 2018. 2, 3
- [25] Yinpeng Dong, Tianyu Pang, Hang Su, and Jun Zhu. Evading defenses to transferable adversarial examples by translation-invariant attacks. In *Proceedings of the IEEE/CVF conference on computer vision and pattern recognition*, pages 4312–4321, 2019. 2
- [26] Yinpeng Dong, Shuyu Cheng, Tianyu Pang, Hang Su, and Jun Zhu. Query-efficient black-box adversarial attacks guided by a transfer-based prior. *IEEE Transactions on Pattern Analysis and Machine Intelligence*, 44(12):9536–9548, 2021. 2
- [27] Yinpeng Dong, Huanran Chen, Jiawei Chen, Zhengwei Fang, Xiao Yang, Yichi Zhang, Yu Tian, Hang Su, and Jun Zhu. How robust is google’s bard to adversarial image attacks? *arXiv preprint arXiv:2309.11751*, 2023. 7, 15
- [28] Alexey Dosovitskiy. An image is worth 16x16 words: Transformers for image recognition at scale. *arXiv preprint arXiv:2010.11929*, 2020. 5, 17
- [29] Alhussein Fawzi, Hamza Fawzi, and Omar Fawzi. Adversarial vulnerability for any classifier. *Advances in neural information processing systems*, 31, 2018. 8
- [30] Stanislav Fort and Balaji Lakshminarayanan. Ensemble everything everywhere: Multi-scale aggregation for adversarial robustness, 2024. 7
- [31] Lianli Gao, Qilong Zhang, Jingkuan Song, Xianglong Liu, and Heng Tao Shen. Patch-wise attack for fooling deep neural network. In *Computer Vision–ECCV 2020: 16th European Conference, Glasgow, UK, August 23–28, 2020, Proceedings, Part XXVIII 16*, pages 307–322. Springer, 2020. 2
- [32] Raphael Gontijo-Lopes, Yann Dauphin, and Ekin D Cubuk. No one representation to rule them all: Overlapping features of training methods. *arXiv preprint arXiv:2110.12899*, 2021. 2
- [33] Ian J Goodfellow. Explaining and harnessing adversarial examples. *arXiv preprint arXiv:1412.6572*, 2014. 1, 2
- [34] Kai Han, Yunhe Wang, Qi Tian, Jianyuan Guo, Chunjing Xu, and Chang Xu. Ghostnet: More features from cheap operations. In *Proceedings of the IEEE/CVF conference on computer vision and pattern recognition*, pages 1580–1589, 2020. 5
- [35] Kaiming He, Xiangyu Zhang, Shaoqing Ren, and Jian Sun. Deep residual learning for image recognition. In *Proceedings of the IEEE conference on computer vision and pattern recognition*, pages 770–778, 2016. 5, 17
- [36] Joel Hestness, Sharan Narang, Newsha Ardalani, Gregory Diamos, Heewoo Jun, Hassan Kianinejad, Md Mostofa Ali Patwary, Yang Yang, and Yanqi Zhou. Deep learning scaling is predictable, empirically. *arXiv preprint arXiv:1712.00409*, 2017. 3
- [37] Andrew G Howard. Mobilenets: Efficient convolutional neural networks for mobile vision applications. *arXiv preprint arXiv:1704.04861*, 2017. 5
- [38] Gao Huang, Zhuang Liu, Laurens Van Der Maaten, and Kilian Q Weinberger. Densely connected convolutional networks. In *Proceedings of the IEEE conference on computer vision and pattern recognition*, pages 4700–4708, 2017. 5
- [39] Hao Huang, Ziyang Chen, Huanran Chen, Yongtao Wang, and Kevin Zhang. T-sea: Transfer-based self-ensemble attack on object detection. In *Proceedings of the IEEE/CVF conference on computer vision and pattern recognition*, pages 20514–20523, 2023. 2, 5
- [40] Yu Huang, Chenzhuang Du, Zihui Xue, Xuanyao Chen, Hang Zhao, and Longbo Huang. What makes multi-modal learning better than single (provably), 2021. 5
- [41] Forrest N Iandola. Squeezenet: Alexnet-level accuracy with 50x fewer parameters and 0.5 mb model size. *arXiv preprint arXiv:1602.07360*, 2016. 5
- [42] Andrew Ilyas, Logan Engstrom, Anish Athalye, and Jessy Lin. Black-box adversarial attacks with limited queries and information. In *International conference on machine learning*, pages 2137–2146. PMLR, 2018. 2
- [43] Andrew Ilyas, Shibani Santurkar, Dimitris Tsipras, Logan Engstrom, Brandon Tran, and Aleksander Madry. Adversarial examples are not bugs, they are features, 2019. 8
- [44] Justin M Johnson and Taghi M Khoshgoftaar. Survey on deep learning with class imbalance. *Journal of big data*, 6(1):1–54, 2019. 5
- [45] Alex K, Ben Hamner, and Ian Goodfellow. Nips 2017: Non-targeted adversarial attack. <https://kaggle.com/competitions/nips-2017-non-targeted-adversarial-attack>, 2017. Kaggle. 5
- [46] Jared Kaplan, Sam McCandlish, Tom Henighan, Tom B. Brown, Benjamin Chess, Rewon Child, Scott Gray, Alec Radford, Jeffrey Wu, and Dario Amodei. Scaling laws for neural language models, 2020. 2, 3

- [47] Alexander Kolesnikov, Lucas Beyer, Xiaohua Zhai, Joan Puigcerver, Jessica Yung, Sylvain Gelly, and Neil Houlsby. Big transfer (bit): General visual representation learning. In *Computer Vision—ECCV 2020: 16th European Conference, Glasgow, UK, August 23–28, 2020, Proceedings, Part V 16*, pages 491–507. Springer, 2020. 5
- [48] Alex Krizhevsky, Geoffrey Hinton, et al. Learning multiple layers of features from tiny images. 2009. 3
- [49] Alex Krizhevsky, Ilya Sutskever, and Geoffrey E Hinton. Imagenet classification with deep convolutional neural networks. *Advances in neural information processing systems*, 25, 2012. 5
- [50] Alexey Kurakin, Ian Goodfellow, and Samy Bengio. Adversarial machine learning at scale. *arXiv preprint arXiv:1611.01236*, 2016. 5
- [51] Christoph H Lampert, Hannes Nickisch, and Stefan Harmeling. Learning to detect unseen object classes by between-class attribute transfer. In *2009 IEEE conference on computer vision and pattern recognition*, pages 951–958. IEEE, 2009. 6
- [52] Yann LeCun, Yoshua Bengio, and Geoffrey Hinton. Deep learning. *nature*, 521(7553):436–444, 2015. 1
- [53] Qizhang Li, Yiwen Guo, Wangmeng Zuo, and Hao Chen. Making substitute models more bayesian can enhance transferability of adversarial examples. *arXiv preprint arXiv:2302.05086*, 2023. 2
- [54] Jiadong Lin, Chuanbiao Song, Kun He, Liwei Wang, and John E Hopcroft. Nesterov accelerated gradient and scale invariance for adversarial attacks. *arXiv preprint arXiv:1908.06281*, 2019. 2
- [55] Chang Liu, Yinpeng Dong, Wenzhao Xiang, Xiao Yang, Hang Su, Jun Zhu, Yuefeng Chen, Yuan He, Hui Xue, and Shibao Zheng. A comprehensive study on robustness of image classification models: Benchmarking and rethinking, 2023. 17
- [56] Haotian Liu, Chunyuan Li, Qingyang Wu, and Yong Jae Lee. Visual instruction tuning, 2023. 5
- [57] Ling Liu, Wenqi Wei, Ka-Ho Chow, Margaret Loper, Emre Gursoy, Stacey Truex, and Yanzhao Wu. Deep neural network ensembles against deception: Ensemble diversity, accuracy and robustness. In *2019 IEEE 16th international conference on mobile ad hoc and sensor systems (MASS)*, pages 274–282. IEEE, 2019. 3
- [58] Yanpei Liu, Xinyun Chen, Chang Liu, and Dawn Song. Delving into transferable adversarial examples and black-box attacks. *arXiv preprint arXiv:1611.02770*, 2016. 2
- [59] Ze Liu, Yutong Lin, Yue Cao, Han Hu, Yixuan Wei, Zheng Zhang, Stephen Lin, and Baining Guo. Swin transformer: Hierarchical vision transformer using shifted windows. In *Proceedings of the IEEE/CVF international conference on computer vision*, pages 10012–10022, 2021. 5, 17
- [60] Zhuang Liu, Hanzi Mao, Chao-Yuan Wu, Christoph Feichtenhofer, Trevor Darrell, and Saining Xie. A convnet for the 2020s. In *Proceedings of the IEEE/CVF conference on computer vision and pattern recognition*, pages 11976–11986, 2022. 5, 17
- [61] Yuyang Long, Qilong Zhang, Boheng Zeng, Lianli Gao, Xianglong Liu, Jian Zhang, and Jingkuan Song. Frequency domain model augmentation for adversarial attack. In *European conference on computer vision*, pages 549–566. Springer, 2022. 2, 4
- [62] Haochen Luo, Jindong Gu, Fengyuan Liu, and Philip Torr. An image is worth 1000 lies: Adversarial transferability across prompts on vision-language models, 2024. 7
- [63] Aleksander Madry. Towards deep learning models resistant to adversarial attacks. *arXiv preprint arXiv:1706.06083*, 2017. 1, 2
- [64] TorchVision maintainers and contributors. Torchvision: Pytorch’s computer vision library. <https://github.com/pytorch/vision>, 2016. 5, 14
- [65] Yichuan Mo, Dongxian Wu, Yifei Wang, Yiwen Guo, and Yisen Wang. When adversarial training meets vision transformers: Recipes from training to architecture, 2022. 17
- [66] OpenAI, Josh Achiam, Steven Adler, Sandhini Agarwal, Lama Ahmad, Ilge Akkaya, Florencia Leoni Aleman, Diogo Almeida, Janko Altschmidt, Sam Altman, Shyamal Anadkat, Red Avila, Igor Babuschkin, Suchir Balaji, Valerie Balcom, Paul Baltescu, Haiming Bao, Mohammad Bavarian, Jeff Belgum, Irwan Bello, Jake Berdine, Gabriel Bernadett-Shapiro, Christopher Berner, Lenny Bogdonoff, Oleg Boiko, Madelaine Boyd, Anna-Luisa Brakman, Greg Brockman, Tim Brooks, Miles Brundage, Kevin Button, Trevor Cai, Rosie Campbell, Andrew Cann, Brittany Carey, Chelsea Carlson, Rory Carmichael, Brooke Chan, Che Chang, Fotis Chantzis, Derek Chen, Sully Chen, Ruby Chen, Jason Chen, Mark Chen, Ben Chess, Chester Cho, Casey Chu, Hyung Won Chung, Dave Cummings, Jeremiah Currier, Yunxing Dai, Cory Decareaux, Thomas Degry, Noah Deutsch, Damien Deville, Arka Dhar, David Dohan, Steve Dowling, Sheila Dunning, Adrien Ecoffet, Atty Eleti, Tyna Eloundou, David Farhi, Liam Fedus, Niko Felix, Simón Posada Fishman, Juston Forte, Isabella Fulford, Leo Gao, Elie Georges, Christian Gibson, Vik Goel, Tarun Gogineni, Gabriel Goh, Rapha Gontijo-Lopes, Jonathan Gordon, Morgan Grafstein, Scott Gray, Ryan Greene, Joshua Gross, Shixiang Shane Gu, Yufei Guo, Chris Hality, Jesse Han, Jeff Harris, Yuchen He, Mike Heaton, Johannes Heidecke, Chris Hesse, Alan Hickey, Wade Hickey, Peter Hoeschele, Brandon Houghton, Kenny Hsu, Shengli Hu, Xin Hu, Joost Huizinga, Shantanu Jain, Shawn Jain, Joanne Jang, Angela Jiang, Roger Jiang, Haozhun Jin, Denny Jin, Shino Jomoto, Billie Jonn, Heewoo Jun, Tomer Kaftan, Łukasz Kaiser, Ali Kamali, Ingmar Kanitscheider, Nitish Shirish Keskar, Tabarak Khan, Logan Kilpatrick, Jong Wook Kim, Christina Kim, Yongjik Kim, Jan Hendrik Kirchner, Jamie Kiros, Matt Knight, Daniel Kokotajlo, Łukasz Kondraciuk, Andrew Kondrich, Aris Konstantinidis, Kyle Kosic, Gretchen Krueger, Vishal Kuo, Michael Lampe, Ikai Lan, Teddy Lee, Jan Leike, Jade Leung, Daniel Levy, Chak Ming Li, Rachel Lim, Molly Lin, Stephanie Lin, Mateusz Litwin, Theresa Lopez, Ryan Lowe, Patricia Lue, Anna Makanju, Kim Malfacini, Sam Manning, Todor Markov, Yaniv Markovski, Bianca Martin, Katie Mayer, Andrew Mayne, Bob McGrew, Scott Mayer McKinney, Christine McLeavey, Paul McMillan, Jake McNeil, David Medina, Aalok Mehta, Jacob Menick, Luke Metz, An-

- drey Mishchenko, Pamela Mishkin, Vinnie Monaco, Evan Morikawa, Daniel Mossing, Tong Mu, Mira Murati, Oleg Murk, David Mély, Ashvin Nair, Reiichiro Nakano, Rajeev Nayak, Arvind Neelakantan, Richard Ngo, Hyeonwoo Noh, Long Ouyang, Cullen O’Keefe, Jakub Pachocki, Alex Paino, Joe Palermo, Ashley Pantuliano, Giambattista Parascandolo, Joel Parish, Emy Parparita, Alex Passos, Mikhail Pavlov, Andrew Peng, Adam Perelman, Filipe de Avila Belbute Peres, Michael Petrov, Henrique Ponde de Oliveira Pinto, Michael, Pokorny, Michelle Pokrass, Vitchyr H. Pong, Tolly Powell, Alethea Power, Boris Power, Elizabeth Proehl, Raul Puri, Alec Radford, Jack Rae, Aditya Ramesh, Cameron Raymond, Francis Real, Kendra Rimbach, Carl Ross, Bob Rotsted, Henri Roussez, Nick Ryder, Mario Saltarelli, Ted Sanders, Shibani Santurkar, Girish Sastry, Heather Schmidt, David Schnurr, John Schulman, Daniel Selsam, Kyla Sheppard, Toki Sherbakov, Jessica Shieh, Sarah Shoker, Pranav Shyam, Szymon Sidor, Eric Sigler, Maddie Simens, Jordan Sitkin, Katarina Slama, Ian Sohl, Benjamin Sokolowsky, Yang Song, Natalie Staudacher, Felipe Petroski Such, Natalie Summers, Ilya Sutskever, Jie Tang, Nikolas Tezak, Madeleine B. Thompson, Phil Tillet, Amin Tootoonchian, Elizabeth Tseng, Preston Tuggle, Nick Turley, Jerry Tworek, Juan Felipe Cerón Uribe, Andrea Vallone, Arun Vijayvergiya, Chelsea Voss, Carroll Wainwright, Justin Jay Wang, Alvin Wang, Ben Wang, Jonathan Ward, Jason Wei, CJ Weinmann, Akila Welihinda, Peter Welinder, Jiayi Weng, Lilian Weng, Matt Wiethoff, Dave Willner, Clemens Winter, Samuel Wolrich, Hannah Wong, Lauren Workman, Sherwin Wu, Jeff Wu, Michael Wu, Kai Xiao, Tao Xu, Sarah Yoo, Kevin Yu, Qiming Yuan, Wojciech Zaremba, Rowan Zellers, Chong Zhang, Marvin Zhang, Shengjia Zhao, Tianhao Zheng, Juntang Zhuang, William Zhuk, and Barret Zoph. Gpt-4 technical report, 2024. [1](#), [2](#), [7](#), [15](#)
- [67] Mark Palatucci, Dean Pomerleau, Geoffrey E Hinton, and Tom M Mitchell. Zero-shot learning with semantic output codes. *Advances in neural information processing systems*, 22, 2009. [6](#)
- [68] Leo Hyun Park, Jaek Kim, Myung Gyo Oh, Jaewoo Park, and Taekyoung Kwon. Adversarial feature alignment: Balancing robustness and accuracy in deep learning via adversarial training, 2024. [17](#)
- [69] ShengYun Peng, Weilin Xu, Cory Cornelius, Matthew Hull, Kevin Li, Rahul Duggal, Mansi Phute, Jason Martin, and Duen Horng Chau. Robust principles: Architectural design principles for adversarially robust cnns, 2023. [17](#)
- [70] Alec Radford and Karthik Narasimhan. Improving language understanding by generative pre-training. 2018. [5](#)
- [71] Alec Radford, Jong Wook Kim, Chris Hallacy, Aditya Ramesh, Gabriel Goh, Sandhini Agarwal, Girish Sastry, Amanda Askell, Pamela Mishkin, Jack Clark, Gretchen Krueger, and Ilya Sutskever. Learning transferable visual models from natural language supervision, 2021. [6](#), [15](#)
- [72] Utkarsh Sharma and Jared Kaplan. Scaling laws from the data manifold dimension. *Journal of Machine Learning Research*, 23(9):1–34, 2022. [3](#)
- [73] Karen Simonyan and Andrew Zisserman. Very deep convolutional networks for large-scale image recognition. *arXiv preprint arXiv:1409.1556*, 2014. [5](#)
- [74] Naman D Singh, Francesco Croce, and Matthias Hein. Revisiting adversarial training for imagenet: Architectures, training and generalization across threat models, 2023. [17](#)
- [75] Xingwu Sun, Yanfeng Chen, Yiqing Huang, Ruobing Xie, Jiaqi Zhu, Kai Zhang, Shuaipeng Li, Zhen Yang, Jonny Han, Xiaobo Shu, Jiahao Bu, Zhongzhi Chen, Xueming Huang, Fengzong Lian, Saiyong Yang, Jianfeng Yan, Yuyuan Zeng, Xiaoqin Ren, Chao Yu, Lulu Wu, Yue Mao, Jun Xia, Tao Yang, Suncong Zheng, Kan Wu, Dian Jiao, Jinbao Xue, Xipeng Zhang, Decheng Wu, Kai Liu, Dengpeng Wu, Guanghui Xu, Shaohua Chen, Shuang Chen, Xiao Feng, Yigeng Hong, Junqiang Zheng, Chengcheng Xu, Zongwei Li, Xiong Kuang, Jianglu Hu, Yiqi Chen, Yuchi Deng, Guiyang Li, Ao Liu, Chenchen Zhang, Shihui Hu, Zilong Zhao, Zifan Wu, Yao Ding, Weichao Wang, Han Liu, Roberts Wang, Hao Fei, Peijie Yu, Ze Zhao, Xun Cao, Hai Wang, Fusheng Xiang, Mengyuan Huang, Zhiyuan Xiong, Bin Hu, Xuebin Hou, Lei Jiang, Jianqiang Ma, Jiajia Wu, Yaping Deng, Yi Shen, Qian Wang, Weijie Liu, Jie Liu, Meng Chen, Liang Dong, Weiwen Jia, Hu Chen, Feifei Liu, Rui Yuan, Huilin Xu, Zhenxiang Yan, Tengfei Cao, Zhichao Hu, Xinhua Feng, Dong Du, Tinghao Yu, Yangyu Tao, Feng Zhang, Jianchen Zhu, Chengzhong Xu, Xirui Li, Chong Zha, Wen Ouyang, Yinben Xia, Xiang Li, Zekun He, Rongpeng Chen, Jiawei Song, Ruibin Chen, Fan Jiang, Chongqing Zhao, Bo Wang, Hao Gong, Rong Gan, Winston Hu, Zhanhui Kang, Yong Yang, Yuhong Liu, Di Wang, and Jie Jiang. Hunyuan-large: An open-source moe model with 52 billion activated parameters by tencent, 2024. [3](#), [7](#), [15](#)
- [76] C Szegedy. Intriguing properties of neural networks. *arXiv preprint arXiv:1312.6199*, 2013. [1](#), [2](#)
- [77] Christian Szegedy, Wei Liu, Yangqing Jia, Pierre Sermanet, Scott Reed, Dragomir Anguelov, Dumitru Erhan, Vincent Vanhoucke, and Andrew Rabinovich. Going deeper with convolutions. In *Proceedings of the IEEE conference on computer vision and pattern recognition*, pages 1–9, 2015. [5](#)
- [78] Christian Szegedy, Vincent Vanhoucke, Sergey Ioffe, Jon Shlens, and Zbigniew Wojna. Rethinking the inception architecture for computer vision. In *Proceedings of the IEEE conference on computer vision and pattern recognition*, pages 2818–2826, 2016. [5](#)
- [79] Mingxing Tan and Quoc Le. Efficientnet: Rethinking model scaling for convolutional neural networks. In *International conference on machine learning*, pages 6105–6114. PMLR, 2019. [5](#)
- [80] Mingxing Tan, Bo Chen, Ruoming Pang, Vijay Vasudevan, Mark Sandler, Andrew Howard, and Quoc V Le. Mnasnet: Platform-aware neural architecture search for mobile. In *Proceedings of the IEEE/CVF conference on computer vision and pattern recognition*, pages 2820–2828, 2019. [5](#)
- [81] Hugo Touvron, Matthieu Cord, Matthijs Douze, Francisco Massa, Alexandre Sablayrolles, and Hervé Jégou. Training data-efficient image transformers & distillation through at-



- tention. In *International conference on machine learning*, pages 10347–10357. PMLR, 2021. 5
- [82] Hugo Touvron, Thibaut Lavril, Gautier Izacard, Xavier Martinet, Marie-Anne Lachaux, Timothée Lacroix, Baptiste Rozière, Naman Goyal, Eric Hambro, Faisal Azhar, et al. Llama: Open and efficient foundation language models. *arXiv preprint arXiv:2302.13971*, 2023. 5
- [83] Florian Tramèr, Alexey Kurakin, Nicolas Papernot, Ian Goodfellow, Dan Boneh, and Patrick McDaniel. Ensemble adversarial training: Attacks and defenses. *arXiv preprint arXiv:1705.07204*, 2017. 5
- [84] Zhengzhong Tu, Hossein Talebi, Han Zhang, Feng Yang, Peyman Milanfar, Alan Bovik, and Yinxiao Li. Maxvit: Multi-axis vision transformer. In *European conference on computer vision*, pages 459–479. Springer, 2022. 5
- [85] Xiaosen Wang and Kun He. Enhancing the transferability of adversarial attacks through variance tuning. In *Proceedings of the IEEE/CVF conference on computer vision and pattern recognition*, pages 1924–1933, 2021. 2
- [86] Zefeng Wang, Zhen Han, Shuo Chen, Fan Xue, Zifeng Ding, Xun Xiao, Volker Tresp, Philip Torr, and Jindong Gu. Stop reasoning! when multimodal llms with chain-of-thought reasoning meets adversarial images. *arXiv preprint arXiv:2402.14899*, 2024. 15
- [87] Ross Wightman. Pytorch image models. <https://github.com/huggingface/pytorch-image-models>, 2019. 5, 14, 15
- [88] Ross Wightman, Hugo Touvron, and Hervé Jégou. Resnet strikes back: An improved training procedure in timm. *arXiv preprint arXiv:2110.00476*, 2021. 5
- [89] Eric Wong, Leslie Rice, and J. Zico Kolter. Fast is better than free: Revisiting adversarial training, 2020. 17
- [90] Mitchell Wortsman, Gabriel Ilharco, Samir Ya Gadre, Rebecca Roelofs, Raphael Gontijo-Lopes, Ari S Morcos, Hongseok Namkoong, Ali Farhadi, Yair Carmon, Simon Kornblith, et al. Model soups: averaging weights of multiple fine-tuned models improves accuracy without increasing inference time. In *International conference on machine learning*, pages 23965–23998. PMLR, 2022. 2
- [91] Haiping Wu, Bin Xiao, Noel Codella, Mengchen Liu, Xiyang Dai, Lu Yuan, and Lei Zhang. Cvt: Introducing convolutions to vision transformers. In *Proceedings of the IEEE/CVF international conference on computer vision*, pages 22–31, 2021. 5
- [92] Cihang Xie, Zhishuai Zhang, Yuyin Zhou, Song Bai, Jianyu Wang, Zhou Ren, and Alan L Yuille. Improving transferability of adversarial examples with input diversity. In *Proceedings of the IEEE/CVF conference on computer vision and pattern recognition*, pages 2730–2739, 2019. 2
- [93] Enze Xie, Wenhai Wang, Zhiding Yu, Anima Anandkumar, Jose M Alvarez, and Ping Luo. Segformer: Simple and efficient design for semantic segmentation with transformers. *Advances in neural information processing systems*, 34:12077–12090, 2021. 5
- [94] Saining Xie, Ross Girshick, Piotr Dollár, Zhuowen Tu, and Kaiming He. Aggregated residual transformations for deep neural networks. In *Proceedings of the IEEE conference on computer vision and pattern recognition*, pages 1492–1500, 2017. 5
- [95] Yifeng Xiong, Jiadong Lin, Min Zhang, John E Hopcroft, and Kun He. Stochastic variance reduced ensemble adversarial attack for boosting the adversarial transferability. In *Proceedings of the IEEE/CVF conference on computer vision and pattern recognition*, pages 14983–14992, 2022. 2
- [96] Jing Xu, Yu Pan, Xinglin Pan, Steven Hoi, Zhang Yi, and Zenglin Xu. Regnet: Self-regulated network for image classification. *IEEE Transactions on Neural Networks and Learning Systems*, 34(11):9562–9567, 2022. 5
- [97] Wei Yao, Zeliang Zhang, Huayi Tang, and Yong Liu. Understanding model ensemble in transferable adversarial attack. *arXiv preprint arXiv:2410.06851*, 2024. 3, 5
- [98] Sergey Zagoruyko. Wide residual networks. *arXiv preprint arXiv:1605.07146*, 2016. 5, 17
- [99] Xiangyu Zhang, Xinyu Zhou, Mengxiao Lin, and Jian Sun. Shufflenet: An extremely efficient convolutional neural network for mobile devices. In *Proceedings of the IEEE conference on computer vision and pattern recognition*, pages 6848–6856, 2018. 5
- [100] Yichi Zhang, Yao Huang, Yitong Sun, Chang Liu, Zhe Zhao, Zhengwei Fang, Yifan Wang, Huanran Chen, Xiao Yang, Xingxing Wei, Hang Su, Yinpeng Dong, and Jun Zhu. Benchmarking trustworthiness of multimodal large language models: A comprehensive study, 2024. 1, 5, 15

## A. Proof of Theorem 1.

As defined in Definition 1,  $\mathbf{x}^*$  is the minimizer of the population loss  $\mathbb{L}(\mathbf{x}) = \mathbb{E}_{f \in \mathcal{F}}[\mathcal{L}(f(\mathbf{x}), \mathbf{y})]$ , and  $\hat{\mathbf{x}}$  is the minimizer of the empirical loss  $\hat{\mathbb{L}}(\mathbf{x}) = \frac{1}{T} \sum_{i=1}^T \mathcal{L}(f_i(\mathbf{x}), \mathbf{y})$ . Thereby we have by gradient equals 0:

$$\nabla \mathbb{L}(\mathbf{x}^*) = \nabla \hat{\mathbb{L}}(\hat{\mathbf{x}}) = 0$$

We use Taylor expansion of  $\nabla \hat{\mathbb{L}}$  at  $\hat{\mathbf{x}}$ :

$$0 = \nabla \hat{\mathbb{L}}(\hat{\mathbf{x}}) = \nabla \hat{\mathbb{L}}(\mathbf{x}^*) + \nabla^2 \hat{\mathbb{L}}(\mathbf{x}^*)(\hat{\mathbf{x}} - \mathbf{x}^*) + \mathcal{O}(\|\hat{\mathbf{x}} - \mathbf{x}^*\|^2).$$

Rearranging, we have:

$$\sqrt{T}(\hat{\mathbf{x}} - \mathbf{x}^*) \approx -\sqrt{T}(\nabla^2 \hat{\mathbb{L}}(\mathbf{x}^*))^{-1} \nabla \hat{\mathbb{L}}(\mathbf{x}^*).$$

From Central Limit Theorem:

$$\begin{aligned} \sqrt{T} \nabla \hat{\mathbb{L}}(\mathbf{x}^*) &= \sqrt{T}(\nabla \hat{\mathbb{L}}(\mathbf{x}^*) - \nabla \mathbb{L}(\mathbf{x}^*)) \\ &\stackrel{d}{\rightarrow} \mathcal{N}(0, \text{Cov}(\mathbb{L}(f_i(\mathbf{x}^*)))), \end{aligned}$$

and the law of large numbers:

$$\nabla^2 \hat{\mathbb{L}}(\mathbf{x}^*) \xrightarrow{P} \nabla^2 \mathbb{L}(\mathbf{x}^*).$$

Plug into the previous equation using  $\mathcal{AN}(0, \Sigma) = \mathcal{N}(0, A\Sigma A^T)$ :

$$\begin{aligned} \sqrt{T}(\hat{\mathbf{x}} - \mathbf{x}^*) &\stackrel{d}{\rightarrow} (\nabla^2 \mathbb{L}(\mathbf{x}^*))^{-1} \mathcal{N}(0, \text{Cov}(\mathbb{L}(f_i(\mathbf{x}^*)))) \\ &\stackrel{d}{=} \mathcal{N}(0, \nabla^2 \mathbb{L}(\mathbf{x}^*)^{-1} \text{Cov}(\mathbb{L}(f_i(\mathbf{x}^*))) \nabla^2 \mathbb{L}(\mathbf{x}^*)^{-1}). \end{aligned}$$

The above indicate  $\hat{\mathbf{x}} - \mathbf{x}^*$  converges in  $\mathcal{O}(\frac{1}{\sqrt{T}})$ .

We can also use Taylor expansion of  $\mathbb{L}$  at  $\mathbf{x}^*$ :

$$\mathbb{L}(\hat{\mathbf{x}}) \approx \mathbb{L}(\mathbf{x}^*) + 0 + \frac{1}{2}(\hat{\mathbf{x}} - \mathbf{x}^*)^T \nabla^2 \mathbb{L}(\mathbf{x}^*)(\hat{\mathbf{x}} - \mathbf{x}^*).$$

Rearranging, we have:

$$\begin{aligned} T(\mathbb{L}(\hat{\mathbf{x}}) - \mathbb{L}(\mathbf{x}^*)) &\approx \frac{1}{2} \sqrt{T}(\hat{\mathbf{x}} - \mathbf{x}^*)^T \nabla^2 \mathbb{L}(\mathbf{x}^*) \sqrt{T}(\hat{\mathbf{x}} - \mathbf{x}^*) \\ &= \frac{1}{2} \|\nabla^2 \mathbb{L}(\mathbf{x}^*) \sqrt{T}(\hat{\mathbf{x}} - \mathbf{x}^*)\|_2^2 = \frac{1}{2} \|S\|_2^2, \end{aligned}$$

where

$$S \sim \mathcal{N}(0, \nabla^2 \mathbb{L}(\mathbf{x}^*)^{-1/2} \text{Cov}(\mathbb{L}(f_i(\mathbf{x}^*))) \nabla^2 \mathbb{L}(\mathbf{x}^*)^{-1/2}).$$

Thus  $T(\mathbb{L}(\hat{\mathbf{x}}) - \mathbb{L}(\mathbf{x}^*))$  converges into a chi-square distribution, which means  $\mathbb{L}(\hat{\mathbf{x}}) - \mathbb{L}(\mathbf{x}^*)$  converges in  $\mathcal{O}(\frac{1}{T})$ .

## B. Experiment Settings for Scaling Laws

In this section we list our models that are included in Sec. 4.2. We select these models based on their diversity in architectures, training methods, and training datasets. Results are shown in Table 3 and Table 4, where all of our models come from open-source platforms such as Torchvision [64] and Timm [87]. Note that *default* in the table means normally trained on ImageNet-1K dataset.

Model name	Architecture	Settings
AlexNet	alexnet	default
DenseNet	densenet121	default
	densenet161	default
	densenet169	default
EfficientNet	efficientnet-b0	default
	efficientnet-b1	default
	efficientnet-b4	default
	efficientnet-v2-s	default
	efficientnet-v2-m	default
	efficientnet-v2-l	default
GoogleNet	googlenet	default
Inception	inception-v3	default
	adv-inception-v3	adversarially trained
	ens-adv-inception-resnet-v2	adversarially trained
MaxVit	maxvit-t	default
MnasNet	mnasnet-0-5	default
	mnasnet-0-75	default
	mnasnet-1-0	default
	mnasnet-1-3	default
MobileNet	mobilenet-v2	default
	mobilenet-v3-s	default
	mobilenet-v3-l	default
RegNet	regnet-x-8gf	default
	regnet-x-32gf	default
	regnet-x-400mf	default
	regnet-x-800mf	default
	regnet-y-16gf	default
	regnet-y-32gf	default
	regnet-y-400mf	default
regnet-y-800mf	default	
ResNet	resnet18	default
	resnet34	default
	resnet50	default
	resnet101	default
	resnet152	default
ShuffleNet	shufflenet-v2-x0.5	default
	shufflenet-v2-x1.0	default
	shufflenet-v2-x1.5	default
	shufflenet-v2-x2.0	default
SqueezeNet	squeezenet-1.0	default
	squeezenet-1.1	default
Vgg	vgg11	default
	vgg11-bn	default
	vgg13	default
	vgg13-bn	default
	vgg16	default
	vgg16-bn	default
	vgg19	default

Table 3. List of pretrained image classifiers that are selected for our model ensemble.

Model name	Architecture	Settings
ViT	vit-b-16	default
	vit-b-32	default
	vit-l-16	default
	vit-l-32	default
	vit-b-16	finetuned on Imagefolder
Wide-ResNet	wide-resnet50-2	default
	wide-resnet101-2	default
BeiT	beit-B-16	trained on ImageNet 21k
GhostNet	ghostnet-100	default
DeiT	deit-B-16	default
LCnet	lcnet-050	default
RepVgg	repvgg-a2	default
DPN	dpn98	default
SegFormer	mit-b0	default
BiT	bit-50	default
CvT	cvt-13	default

Table 4. List of pretrained image classifiers that are selected for our model ensemble (continued).

### C. Test Prompts as Metrics

As VLMs and MLLMs output prompts rather than logits, we evaluate the attack efficacy by mainly focusing on the “classification” results of the test models, which is leveraging a GPT4 assistant to judge the content of the test models’ descriptions. We develop **Metric 1** and **Metric 2**, focusing on different aspects of the descriptions.

Fig. 7a and Fig. 7b display our prompts for Metric 1 and Metric 2 respectively. Metric 1 follows the settings in previous works [100], while Metric 2 is our customized metric to capture image features, as stated in Sec. 5.2. By comparing the results in Fig. 5 and Table. 2, Metric 2 have a 10% higher success rate than Metric 1 under  $\epsilon = 8/255$  cases. This phenomenon is natural since some images of high noise will be still considered as success in Metric 2, which is more aligned with our practical approaches [27].

### D. Experiment Results for MLLMs

In Table 5 we list the 12 CLIPs that are collected for our model ensemble, which are all open-source models selected from OpenAI [71], OpenCLIP [15], and Timm [87]. We select 6 commercial MLLMs as our black-box test models - GPT-4o, GPT-4 Turbo [66], Claude-3.5 Sonnet ‡, Gemini-1.5 Pro §, Hunyuan [75], Qwen [6] - and 3 open-source

‡<https://www.anthropic.com/news/claude-3-family>  
§<https://deepmind.google/technologies/gemini/pro/>

Model Name	Architecture	Datasets
ViT-L OpenAI	ViT-L-14	WebImageText
ViT-B LAION-2B	ViT-B-32	LAION-2B
ViT-B LAION-2B	ViT-B-16	LAION-2B
ViT-bigG LAION-2B	ViT-bigG-14	LAION-2B
ViT-g LAION-2B	ViT-g-14	LAION-2B
ViT-H LAION-2B	ViT-H-14	LAION-2B
ViT-L LAION-2B	ViT-L-14	LAION-2B
ConvNeXt-L LAION-2B	ConvNeXt-large-d-320	LAION-2B
ViT-B DataComp	ViT-B-16	DataComp-1B
ViT-B DataComp	ViT-B-32	DataComp-1B
ViT-L DataComp	ViT-L-14	DataComp-1B
SigLip WebLI	ViT-SO400M-14-SigLIP	WebLI

Table 5. List of CLIPs that are selected as model ensemble.

MLLMs - LLama-3.2 90B ¶, Pixtral Large ¶, and DeepSeek-VL 7B [19]. In Table 2 we only list part of the results for better demonstration of our capability in creating powerful adversarial examples, therefore in Table 6 we list experiment results for rest of these models. From the results we observe that the high attack success rates of our adversarial examples are generalized results, and the transferability of our adversarial examples is strong enough to fool most popular MLLMs. Compared to previous methods that tried to attack commercial MLLMs by visual adversarial examples [27], our methods exhibit a 40% higher success rate. This demonstrates the strength of our core inspiration of scaling, and highlights the practical applications of our methods. Meanwhile, we find the recently released open-source models *Llama-3.2 90B* and *Pixtral Large* exhibiting a better performance than other models generally, which indicates that the AI community is running towards developing more robust, safe and reliable MLLMs.

### E. Degenerated Image Generation Task

As stated in Sec. 6.1, when  $\epsilon$  goes larger, the adversarial attack task degenerates to an image generation task. Previous works [3, 13, 86] do not ever think about this field, but we believe that adversarial attack task and image generation task are indeed homogenous. We display our adversarial examples generated from 64 image classifiers (stated in Appendix B) under  $\epsilon = 64/255$  in Fig. 8. From the visualizations we observe that our methods can capture the key features of the target class and reproduce them based on the original textures of images. This visualization further supports our methods are really attacking common weakness instead of running into local optima. We leave further explorations and analyses as future work.

¶<https://ai.meta.com/blog/llama-3-2-connect-2024-vision-edge-mobile-devices/>

¶<https://mistral.ai/news/pixtral-large/>

**Prompt for Testing Accuracy:**

Given a chatbot's description of a scene:[response]. Is it stated in the description that there is a/an [target]? Please answer 'Yes.' or 'No.'

**Prompt for Judging Image Quality:**

Given a chatbot's description of an image: '[response]'. Does the description mention factors that affect the judgment of the image content, such as low image quality, noise, or modification? Please answer 'Yes.' or 'No.'

(a) Prompts for Metric 1.

**Prompt for Testing Accuracy:**

Given the above description, does this description talk about or mention a/an [target]? You can only answer 'Yes.' or 'No.'

(b) Prompt for Metric 2.

Figure 7. Prompts of two metrics. (a) Besides prompt to test the adversarial example contain a target label, we also use a prompt to judge the image quality, ensuring our successful attacks are all of small noise and highly transferable. (b) The prompt concentrates on semantic meanings of the image descriptions. To consider the attack successful, it only needs the target to appear in the description.

ASR(%)	Target: Cat		Target: Car		Target: Ship		Target: Deer		Target: Bird	
$\epsilon$ ( $\ell_\infty$ norm)	8/255	16/255	8/255	16/255	8/255	16/255	8/255	16/255	8/255	16/255
Gemini-1.5 Pro	0.4	<b>0.92</b>	0.16	<b>0.50</b>	0.35	<b>0.82</b>	0.29	<b>0.82</b>	0.38	<b>0.83</b>
Hunyuan-Vision	0.58	<b>0.95</b>	0.23	<b>0.53</b>	0.59	<b>0.90</b>	0.42	<b>0.88</b>	0.52	<b>0.95</b>
Qwen-VL Plus	0.75	<b>0.98</b>	0.28	<b>0.54</b>	0.65	<b>0.91</b>	0.52	<b>0.92</b>	0.69	<b>0.97</b>
Llama-3.2 90B	0.48	<b>0.88</b>	0.21	<b>0.48</b>	0.42	<b>0.87</b>	0.39	<b>0.87</b>	0.4	<b>0.86</b>
Pixtral Large	0.49	<b>0.88</b>	0.19	<b>0.49</b>	0.46	<b>0.87</b>	0.36	<b>0.77</b>	0.44	<b>0.87</b>
Deepseek-VL 7B	0.54	<b>0.96</b>	0.17	<b>0.52</b>	0.52	<b>0.87</b>	0.44	<b>0.91</b>	0.51	<b>0.93</b>

Table 6. ASR under Metric 2 measured across different settings of  $\epsilon$ . Following Table 2, we extend our evaluations to most popular models (both commercial and open-sourced) to obtain more generalized results.

### F. Results on Adversarially Trained Models

We provide our experiment settings and results for Sec. 6.2. We still adapt the adversarial examples generated from nor-

mal image classifiers and test them on adversarially trained models, as in Sec. 4.3.

**Black-box Test Models:** We select 9 pretrained models from robustbench [16] leading board with different archi-





Figure 8. Visualizations of adversarial examples under  $\epsilon = 64/255$ . The adversarial examples capture basic information of the target class, such as the fur of cats, tires of vehicles, cargo on ships, antlers of deer, and feathers of birds.

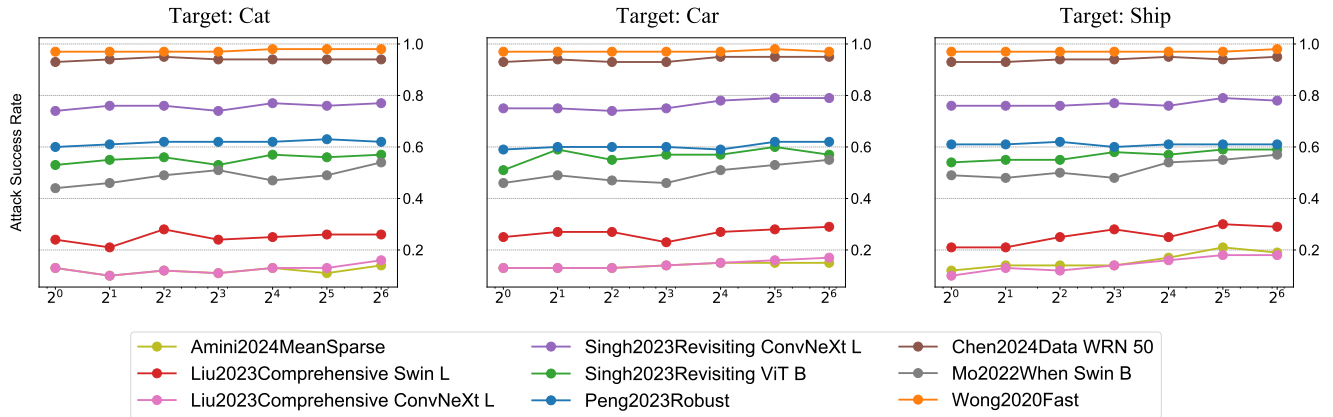


Figure 9. Results on attacking adversarially trained models in the untargeted metric setting. No obvious scaling trends can be observed from the results, and the attack success rate remains consistent regardless of ensemble cardinality.

tectures and defense methods - architectures include ResNet [35], Swin-Transformers [59], ConvNeXt [60], ViT [28] and Wide-ResNet [98], while defense methods include Mean-Centered feature sparsification [2], designing better benchmarks [55], combining with ConvStem architecture [74], incorporating with generalizable design principles [69], data filtering [12], randomly masking gradients [65], and using FGSM optimizer during adversarial training [89]. By selecting these models as test subjects, we ensure that a sufficient variety of defense mechanisms are represented, allowing us to draw reliable conclusions.

**Evaluation Metrics:** Since adversarially trained models typically incorporate defense strategies against adversarial examples, we adjust our evaluation approach. Specifically, we measure the attack success rate based on whether the test models classify the adversarial examples differently from the natural images, a widely used method in untargeted attack evaluations.

As we observe from Fig. 9, a larger model ensemble does not indicate a higher transfer attack success rate. Instead,

under our untargeted attack metric, the attack success rate remains consistent across all adversarially trained models. This reveals the fact that scaling laws do not hold over adversarially trained models. By visualizations in Sec 6.2, we claim this is because the gap between normal image classifiers and adversarially trained classifiers on image understanding. Adversarially trained classifiers have a completely different focus on image features, making them insensitive to attack patterns crafted from normal image classifiers. The results show scaling laws only exist when models are sampled from similar data distribution (i.e. normal datasets that are sampled from physical world or training methods that do not exclude specific features of the data), which supports the assumption in Sec. 4.1 of i.i.d. models. Meanwhile, though the attack success rate only slightly changes with ensemble cardinality, we observe from Fig. 9 that many adversarially trained models have bad classification accuracy. This is because adversarially trained models try to strike a balance between accuracy and robustness [68], therefore losing accuracy under small noise.